Modeling the Flowability of Granular Materials

by

Cameron Kleppe

A Thesis Presented in Partial Fulfillment
of the Requirements for the Degree
Master of Science

Approved November 2019 by the
Graduate Supervisory Committee:

Heather Emady, Chair
Hamidreza Marvi
Shuguang Deng

ARIZONA STATE UNIVERSITY

December 2019

ABSTRACT

This thesis investigated the effects of differing diameters and varying moisture content on the flowability properties of granular glass beads through use of a Freeman FT4 Powder Rheometer. These parameters were tested in order to construct an empirical model to predict flowability properties of glass beads at differing size ranges and moisture contents. The final empirical model outputted an average error of 8.73% across all tested diameters and moisture ranges.

Mohr's circles were constructed from experimentally-obtained shear stress values to quantitatively describe flowability of tested materials in terms of a flow function parameter. A high flow function value (>10) was indicative of a good flow.

By testing 120-180 µm, 120-350 µm, 180-250 µm, 250-350 µm, 430-600 µm, and 600-850 µm glass bead diameter ranges, an increase in size was seen to result in higher flow function values. The limitations of testing using the FT4 became apparent as inconsistent flow function values were obtained at 0% moisture with size ranges above 120-180 µm, or at flow function values of >21. Bead sizes larger than 430 µm showed significant standard deviation over all tested trials--when excluding size ranges above that value, the empirical model showed an average error of only 6.45%.

Wet material testing occurred at all tested glass bead size ranges using a deionized water content of 0%, 1%, 5%, 15%, and 20% by weight. The results of such testing showed a decrease in the resulting flow function parameter as more water content was added. However, this trend changed as 20% moisture content was achieved; the wet material became supersaturated, and an increase in flow function values was observed. The empirical model constructed, therefore, neglected the 20% moisture content regime.

TABLE OF CONTENTS

Page

LIST OF TABLES iv

LIST OF FIGURES v

CHAPTER

1 INTRODUCTION 1

Background 1

Apparatus 3

Mohr's Circles 5

2 MATERIALS & METHODS 8

3 RESULTS 10

Comparison of Dry Bead Data at Varying Bead Sizes 10

Comparison of Wet Bead Data 11

Construction of Empirical Model 17

4 CONCLUSIONS 20

REFERENCES 23

APPENDIX

A MOHR'S CIRCLES USED FOR FLOW FUNCTION CALCULATION 24

LIST OF TABLES

Table Page

1. Flow Function Values at Each Glass Bead Diameter Range 11

2. Flow Function Values at Each Tested Moisture Content 15

3. Percent Error between Experimental and Theoretical Flow Function Values 19

LIST OF FIGURES

Figure Page

1. An Example of Shear Stress on a Powder Bed with an Applied Normal Stress ...2
2. The Rotational Shear Testing Method Utilized by the FT4 Powder Rheometer ..5
3. Mohr's Circles Applied to a Yield Locus for Flow Function Calculation 6
4. Results of Shear Stress Testing on Dry Glass Beads of Various Diameters 10
5a. 120-180 µm Glass Beads Tested at Various Levels of Moisture Content 12
5b. 180-250 µm Glass Beads Tested at Various Levels of Moisture Content 12
5c. 250-350 µm Glass Beads Tested at Various Levels of Moisture Content 13
5d. 430-600 µm Glass Beads Tested at Various Levels of Moisture Content 13
5e. 600-850 µm Glass Beads Tested at Various Levels of Moisture Content 14
6. FF Values at Each Tested Moisture Content and Size Range of Glass Beads 16
7. Power Functions Applied to Figure 6 17
8. Values Leading the Power Functions vs. Bead Diameter 18

CHAPTER 1

INTRODUCTION

Background

Granular materials are quite complex and properties relatively unknown— for example, the bulk mass can remain stationary on a flat plane as would solids, but if the plane were inclined, liquid-like flow would occur.[1] These materials cannot be properly described by statistical mechanics; temperature is not significant, and particles collisions are inelastic.[2] Due to these behaviors, characterizing granular properties is quite difficult, especially with the addition of other variables (such as added moisture content). However, characterizing these granular material properties is essential in achieving reliable flow in many particulate processing operations, especially those that utilize hoppers.[3] A need to characterize such properties on a wet basis is required by processes dealing with wet materials.[4,5]

Shear stress is a property that can be quantified to determine quality of flow and improve inherent design in particulate processes. When a material's shear strength is overcome by shear forces (those parallel to the plane on which the powder resides), the top layer of the powder bed will slide over the lower, such as in Figure 1. At this point, the material will begin to flow. Materials with high shear strength will be more resistant to yielding and beginning to flow at a given value of shear stress (the shear force over an applied area); therefore, a higher value of shear stress must be used.[5]

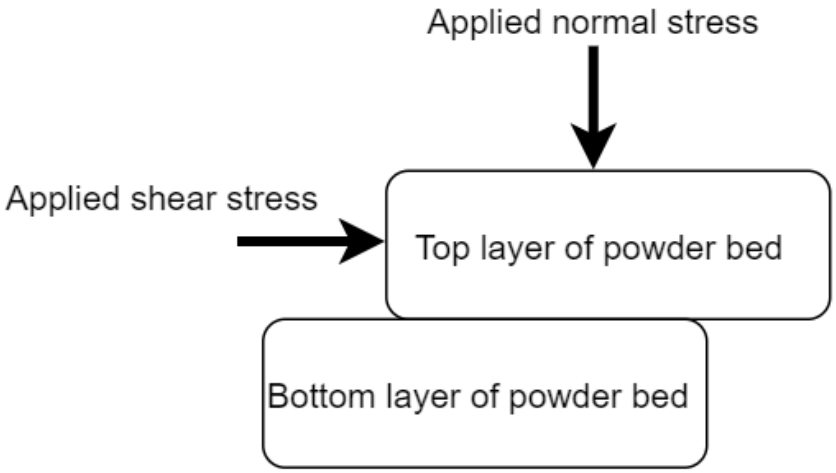

Figure 1: An Example of Shear Stress on a Powder Bed with an Applied Normal Stress.[6]

Often, the applied shear stress required for flow to begin is obtained at various applied normal stresses. By developing relationships between these two properties, a flowability value can be derived to quantitatively describe the goodness of flow. With such flowability values known, reliable flow can be obtained in particulate processes and design improvements can be made.

This is a continuation of the research done in a prior Barrett thesis, which had begun to quantify the flowability values at various diameters and delve into the testing of wet materials.[5] The current study completed wet material testing and used the resulting data to form an empirical equation able to predict flowability values at various glass bead diameter ranges and moisture ranges with a small degree of error (8.73% amongst all materials or 6.45% when excluding larger materials).

Collisions between spherical particles can result in the buildup of electrostatic forces. These forces may cause the beads to adhere to other beads or the surface of the testing vessel. It was hypothesized in the prior Barrett thesis that obtained shear stress

values at applied normal stresses (and therefore the quantified flowability of the material) may be affected by the presence of these adhesive forces, which led to testing material shear properties with an antistatic solution mixed into the sample. The results were compared to a control group (materials without an antistatic solution). For the ranges of glass beads utilized in this thesis, research from the prior Barrett thesis showed that antistatic forces were not significant.[5] However, if smaller size ranges were to be tested (below 120 μm), due cause would exist to again test for antistatic forces.

Apparatus

A Freeman FT4 Powder Rheometer was used to test for the applied shear stresses necessary to begin flow in materials at varying levels of applied normal stress. This rheometer was chosen due to its capability of recreating conditions observable in actual particulate processes. It does so by utilizing three independent steps: a conditioning cycle, a compression phase, and a shearing cycle.[1]

During the conditioning cycle, a small blade is inserted into the testing vessel and rotated while slowly moving vertically throughout the whole of the sample bed. This creates uniformity throughout the sample by both displacing and aerating the whole of the powder bed, eliminating possible errors caused by uneven loading of material sample (which is done by hand by the operator). A vented piston then replaces the conditioning blade, and the sample is then subjected to an increasing level of compressive normal force. The piston vents allow the escape of any trapped air. A rotating shear cell is then used for data collection of applied shear stress values at various levels of applied normal

stress. The incorporation of all three steps is ideal in eliminating deviation potentially caused by human error.[1,5]

Typically, obtaining shear stress values at which the powder will begin to flow are done through translational means; a common method is the use of a Jenike cell. This method incorporates physically splitting the upper and lower layers of the powder bed by applying shear stress at a known quantity of applied normal stress (such as in Figure 1). This dynamic method would consume more equipment space than does the rotational method utilized by the FT4 (seen in Figure 2). Additionally, translational methods often require new trials at every value of applied normal stress. By utilizing a novel rotational method, the FT4 allows the shear stress values of a sample to be obtained at many values of applied normal stress within the span of a single trial.[1,5]

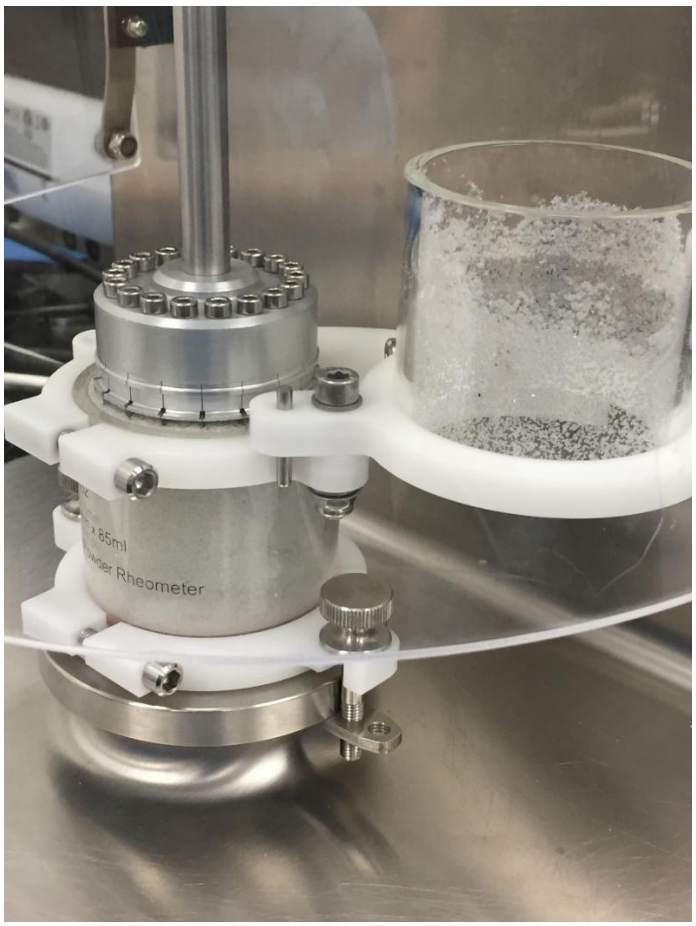

Figure 2: The Rotational Shear Testing Method Utilized by the FT4 Powder Rheometer.

Mohr's Circles

Applied shear stress values at various levels of applied normal stress at which a powder would yield and begin to flow are outputted by imbedded data analysis software from the FT4; these are the values obtained by testing using the shear cell component. A yield locus results from plotting the applied shear stress vs. applied normal stress values. From these yield loci, Mohr's circles are constructed (such as in Figure 3), representing possible combinations of various stress components where the material tested would be expected to fail and flow to begin.[5,7]

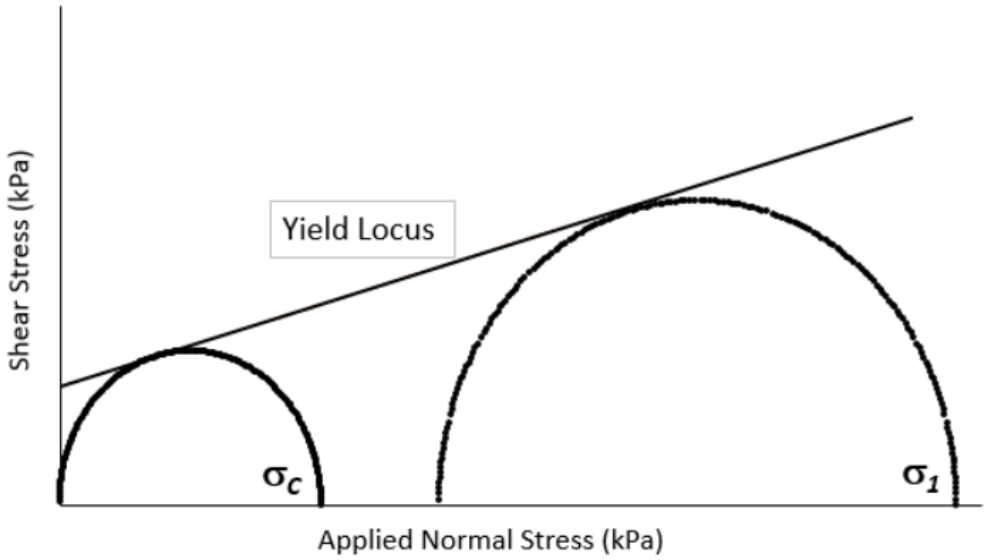

Figure 3: Mohr's Circles Applied to a Yield Locus for Flow Function Calculation.

The unconfined yield strength, σ_C, represents the maximum principal stress a system can withstand before flow begins. This value is obtained by creating a Mohr's circle from the origin; the top half of the circle remains within the positive quadrant of the plot, and it tangentially touches the yield locus. The unconfined yield strength is then obtained as the point at 0 kPa of applied shear stress at the maximum principal normal stress of the smaller Mohr's circle. The major consolidated stress of the system, σ_1, is obtained by creating a Mohr's circle tangent to both the yield locus and to the initial point of testing of the system (in this case, consolidation at 9 kPa). This parameter is the major principal stress of the system when steady-state flow is obtained.[5,7]

Flow function, FF, uses both the unconfined yield strength and the major consolidated stress of the system in order to quantitatively denote flowability, or goodness of flow.[1]

$$FF = \frac{\sigma_1}{\sigma_C} \tag{1}$$

Here, σ_1 represents the major consolidated stress, and σ_C represents the unconfined yield strength. A flow function value below 4 signifies poor or cohesive flow, while a flow function value between 4 and 10 denotes easy flow. A flow function value above 10 signifies very good flow; at this value, the material is considered free-flowing.[5,8]

Characterizing flow is essential in the design of hoppers, which are used in nearly all industries that conduct particulate processing. The unconfined yield strength from Mohr's circles is critical in preventing ratholing, and the flow function parameter is often used in calculations to prevent arching within hopper design.[9]

CHAPTER 2

MATERIALS & METHODS

Spherical glass beads were used as they are a standard baseline material, behaving more ideally than most powders. Shear stress values at various applied values of normal stress with moisture contents of 0%, 1%, 5%, 15%, and 20% (water-by-weight) were obtained for five glass bead size ranges: 120-180 µm, 180-250 µm, 250-350 µm, 430-600 µm, and 600-850 µm. An additional mixed range of 120-350 µm was tested at 0% moisture content; this sample size was prepared by combining equivalent masses of 120-180 and 250-350 µm glass beads into a Ziploc bag and mixing via both shaking and kneading for 5 minutes.[5]

To prepare materials for testing with moisture content added, 200 grams of a chosen glass bead size range and the desired amount of deionized water were combined in a Ziploc bag and kneaded for 10 minutes. Wet materials were prepared immediately before testing in order to negate possible effects of evaporation.[5]

Prepared samples were packed into a 50 mm diameter cylindrical testing vessel attached to the FT4. A 48 mm diameter vented piston was attached and used during a compression phase, rising from 0 to 9 kPa and concluding once a time-based steady-state criteria was met. The testing vessel was then split; the contents in the upper half were discarded, and the contents in bottom half of the vessel (85 mL of material) remained to undergo shear testing. The vented piston was removed, and a 48 mm diameter shear cell (observed in Figure 2) was then attached.[5]

Shear stress testing began by consolidating the material at an applied normal force value of 9 kPa. Once a steady-state exit criteria was met, the shear cell returned to 0 kPa

and then rose to 7 kPa of applied normal force. The shear stress value was recorded, then 0 kPa force applied prior to rising to 6 kPa. This occurred from 7 kPa to 3 kPa in increments of 1 kPa, and the stress values were recorded in the data analysis software at each interval. Three trials were conducted with each size range at each value of moisture content.[5]

The default program for shear cell testing utilizes a conditioning cycle prior to the compression phase. This, however, was not used, because wet material would still be attached to the conditioning blade as it left the testing vessel; the FT4 would show an error message, and the test would abort. To prevent this error, the test was programmed to only utilize the compression phase and the shear cell cycle.[4] Additionally, the default shear cell testing program demanded 10 pre-shears at 9 kPa (or two consecutive pre-shears reaching within 99% of the same shear stress value) prior to actual testing. This was not ideal for wet materials as the initial pre-shears would significantly displace the cohesive material, causing no two consecutive pre-shears to be within 99% of the same value. The program would then perform the maximum 10 pre-shears at the beginning of every trial. This led to significant material displacement, causing data obtained during the actual testing phase to deviate significantly and rarely result in the linear slope needed to form a yield locus. Therefore, the program was modified to have a maximum of 4 pre-shears, or two consecutive within 97% of the same shear stress value.

CHAPTER 3

RESULTS

Comparison of Dry Bead Data at Varying Bead Sizes

Glass beads with diameters of 120-180 µm, 120-350 µm, 180-250 µm, 250-350 µm, 430-600 µm, and 600-850 µm were tested at 0% moisture content in order to compare the effects of varying bead diameter on flow properties. The yield loci resulting from testing can be seen in Figure 4.

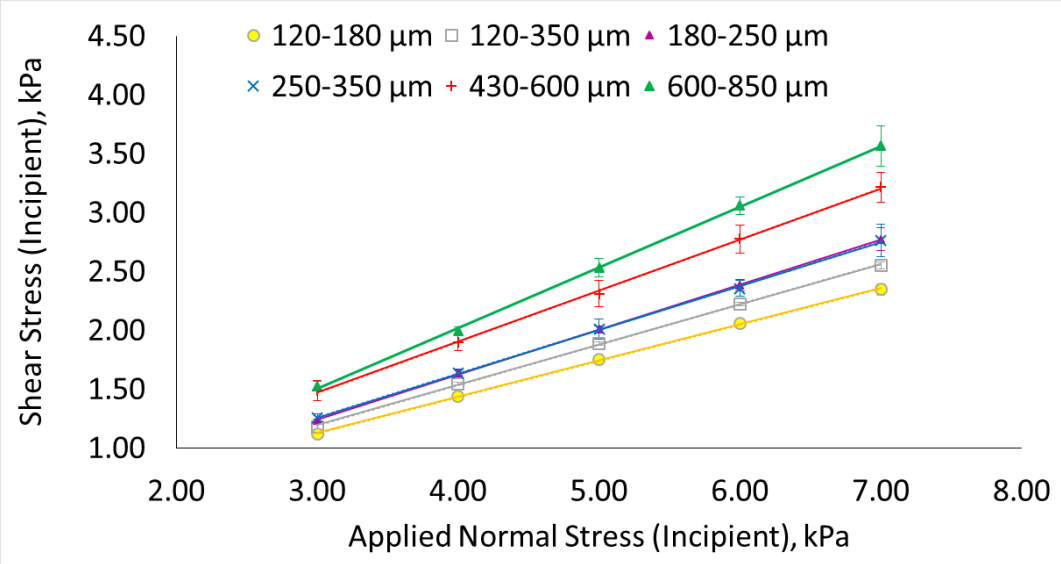

Figure 4: Results of Shear Stress Testing on Dry Glass Beads of Various Diameters.

Figure 4 shows that as the diameter of the beads increased, the applied shear stress values necessary for the material to yield at each level of applied normal stress also increased. An increase in both slope and standard deviation was also observed as the bead diameter size was increased.

From these yield loci, Mohr's circles were plotted, and the major consolidated stress and unconfined yield strength values were obtained. The calculated flow function value for each glass bead diameter range is seen in Table 1.

Table 1: Flow Function Values at Each Glass Bead Diameter Range

Glass Bead Diameter (mm)	Flow Function (FF) at 0% Moisture
0.12-0.18	20.4
0.12-0.35	24.4
0.18-0.25	22.6
0.25-0.35	29.7
0.43-0.60	34.1
0.60-0.85	47.7

Flow function was observed to increase with increasing diameter size, and the 120-350 µm mixed range appropriately yielded a flow function value between that of the 120-180 and 250-350 µm ranges. The flow function values obtained all showed very good flowability at these size ranges; each yielded a FF value greater than 20.

Comparison of Wet Bead Data

The 120-180 µm, 180-250 µm, 250-350 µm, 430-600 µm, and 600-850 µm ranges of glass beads were used in wet material testing. Tested moisture contents included 0%, 1%, 5%, 15%, and 20% water-by-weight. The results can be seen in Figures 5a, 5b, 5c, 5d, and 5e.

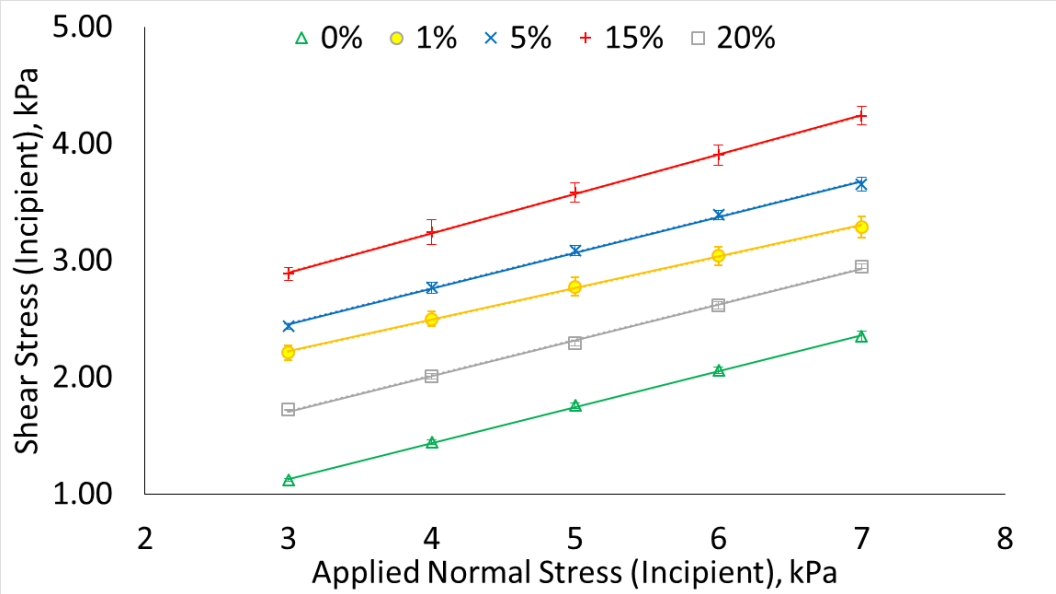

Figure 5a: 120-180 µm Glass Beads Tested at Various Levels of Moisture Content.

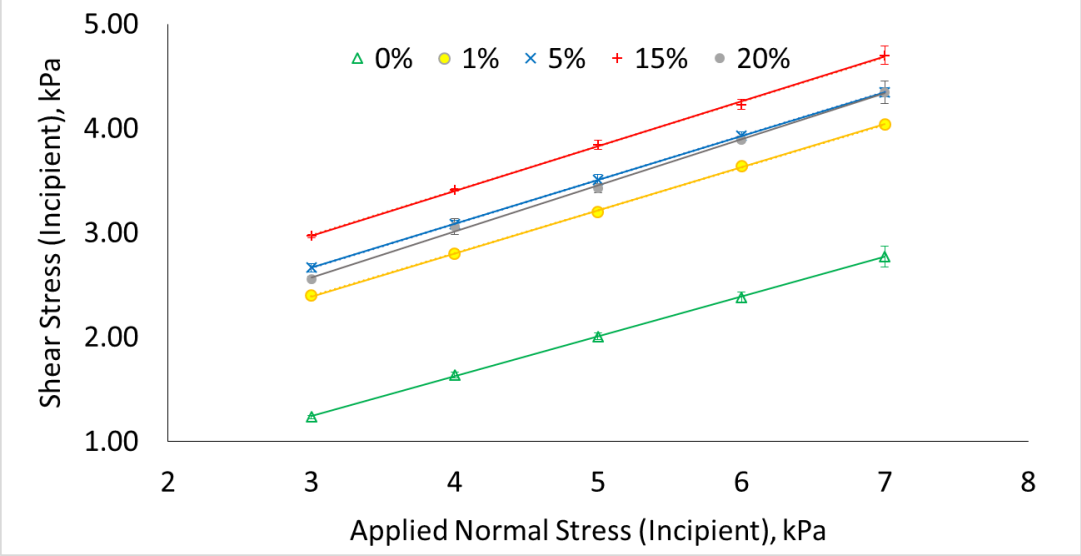

Figure 5b: 180-250 µm Glass Beads Tested at Various Levels of Moisture Content.

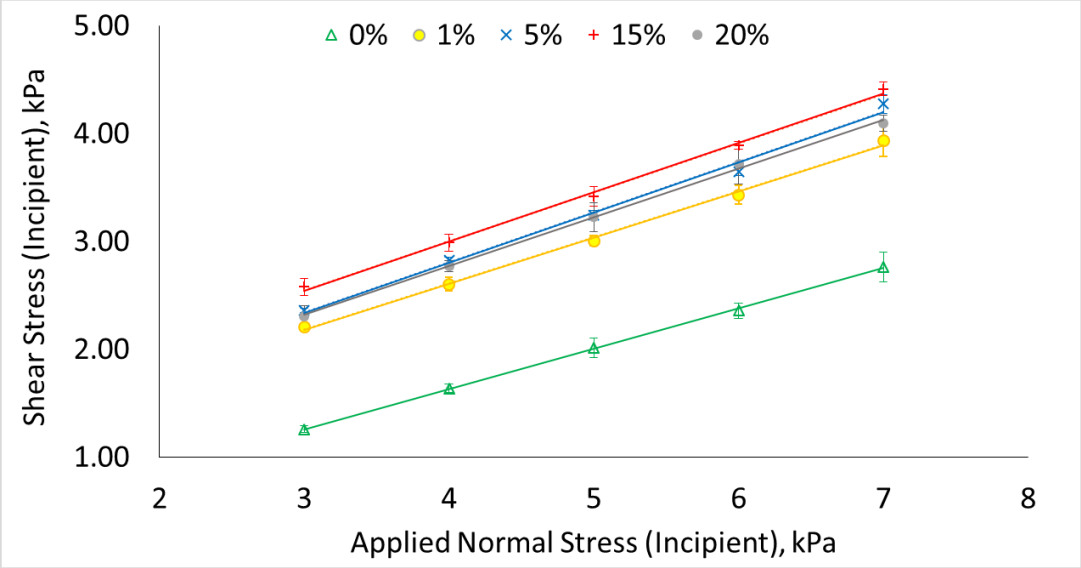

Figure 5c: 250-350 µm Glass Beads Tested at Various Levels of Moisture Content.

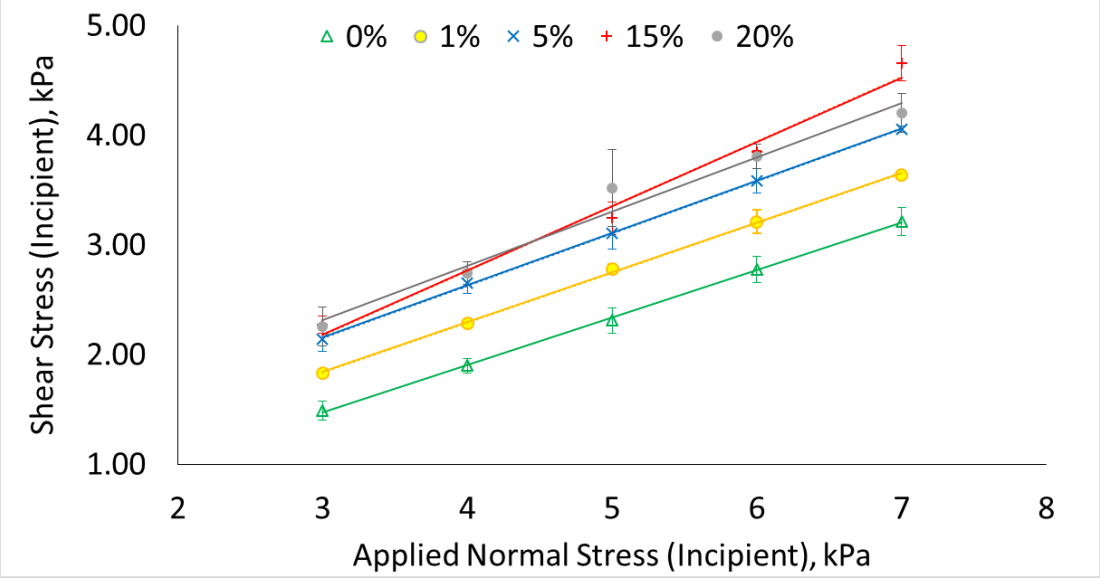

Figure 5d: 430-600 µm Glass Beads Tested at Various Levels of Moisture Content.

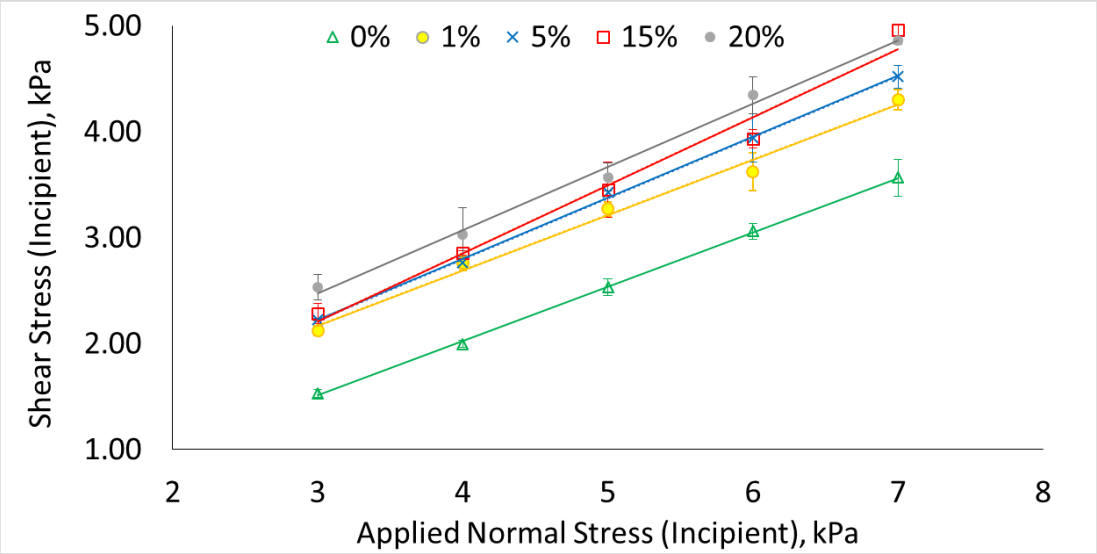

Figure 5e: 600-850 µm Glass Beads Tested at Various Levels of Moisture Content.

As seen in Figures 5a, b, c, d, and e, glass beads of all tested size ranges were observed to increase in applied shear stress values at varying applied normal stress values as the percentage of moisture content was increased. This held true for all moisture contents except 20%, when the shear stress values dropped below those observed at 15% moisture content for all size ranges of beads except the 600-850 µm range. Notably, the difference in shear stress values obtained when increasing from 0% to 1% moisture content was significantly larger than the difference observed when increasing from 1% to higher moisture contents. The slope appeared to be relatively constant at each given size range as moisture content was increased, whereas the slope was observed to increase significantly when bead diameter was increased in Figure 4.

Figures 5d and 5e showed significant standard deviation at larger sizes of tested glass beads with high quantities of moisture added. At 6 kPa and 7 kPa values of applied normal stress, more moisture content (particularly 15% and 20%) yielded poor data in the

plots for the 430-600 µm and 600-850 µm diameter beads; large amounts of standard deviation were observed between trials. This was because the system failed to reach a steady-state due to not enough pre-shears occurring. This highlights the limitations of testing larger sizes of cohesive materials with the FT4, as too many pre-shears can displace the cohesive material and cause significant standard deviation in testing or the FT4 to error out and not finish testing at all.

Flow function values were obtained at each size range and moisture content tested via Mohr's circles.

Table 2: Flow Function Values at Each Tested Moisture Content.

Glass Bead Diameter (mm)	Moisture Content				
	0%	1%	5%	15%	20%
0.12-0.18	20.4	3.43	3.16	2.64	5.78
0.18-0.25	22.6	3.90	3.25	2.76	3.62
0.25-0.35	29.7	4.89	4.58	3.77	4.59
0.43-0.60	34.1	8.69	5.96	5.26	5.32
0.60-0.85	47.7	9.67	8.40	7.55	8.69

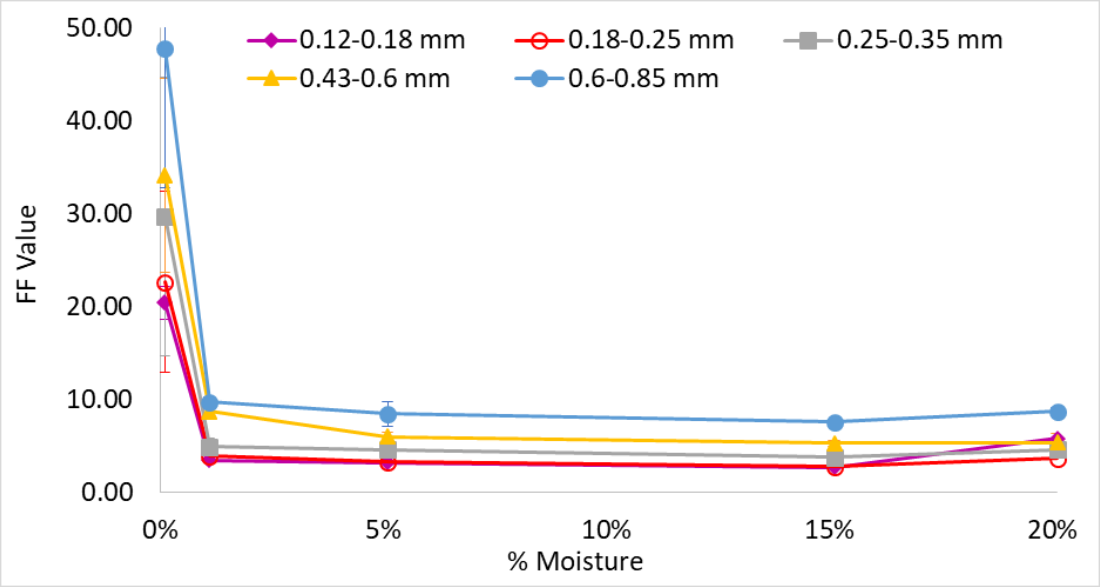

Figure 6: FF Values at Each Tested Moisture Content and Size Range of Glass Beads.

Figure 6 (quantified in Table 2) shows a large decrease in flow function from 0% to 1% moisture content (an inverse to the increasing relationship seen in the shear stress vs. applied normal force plots in Figures 5a, b, c, d, and e). Flow function continued to decrease slightly until 20% moisture content, where instead a slight increase in flow function was observed as the material became supersaturated with water.

The standard deviation seen at the 0% moisture range in Figure 6 was significantly larger than that observed at higher moisture contents. This deviation, however, was significantly smaller at the 120-180 µm range, where the average flow function across all 3 trials was 20.4. All larger size ranges showed flowability values greater than 21 at 0% moisture and did not show large standard deviations at moisture values greater than 0% (where the flow function was significantly less than 21). The FT4,

therefore, was ideal for testing materials under a flow function value of 21; above this, the deviation from trial-to-trial was too large.

Construction of Empirical Model

In order to construct an empirical model of the data to predict flow function values at various size ranges and moisture contents, the plot in Figure 6 was recreated to exclude values at 20% moisture content. This was done in order to model based on a power function, which would not be able to account for the increase in flowability observed at 20% moisture content.

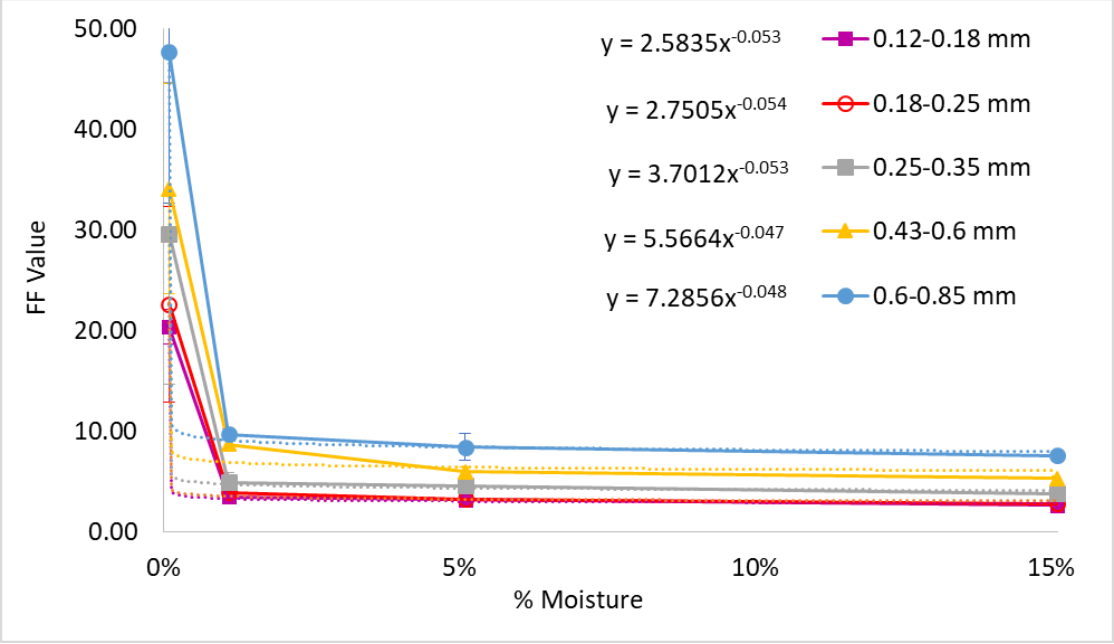

Figure 7: Power Functions Applied to Figure 6.

Figures 5d and 5e highlighted the inability of the FT4 to effectively test cohesive material at sizes greater than 430 µm. Therefore, the power function $x^{-0.053}$ obtained in

Figure 7 was utilized in the final empirical equation as the functions observed at the 430-600 µm and 600-850 µm diameter ranges were considered outliers.

The values in front of the power function vs. the mean values of each size range were plotted in Figure 8.

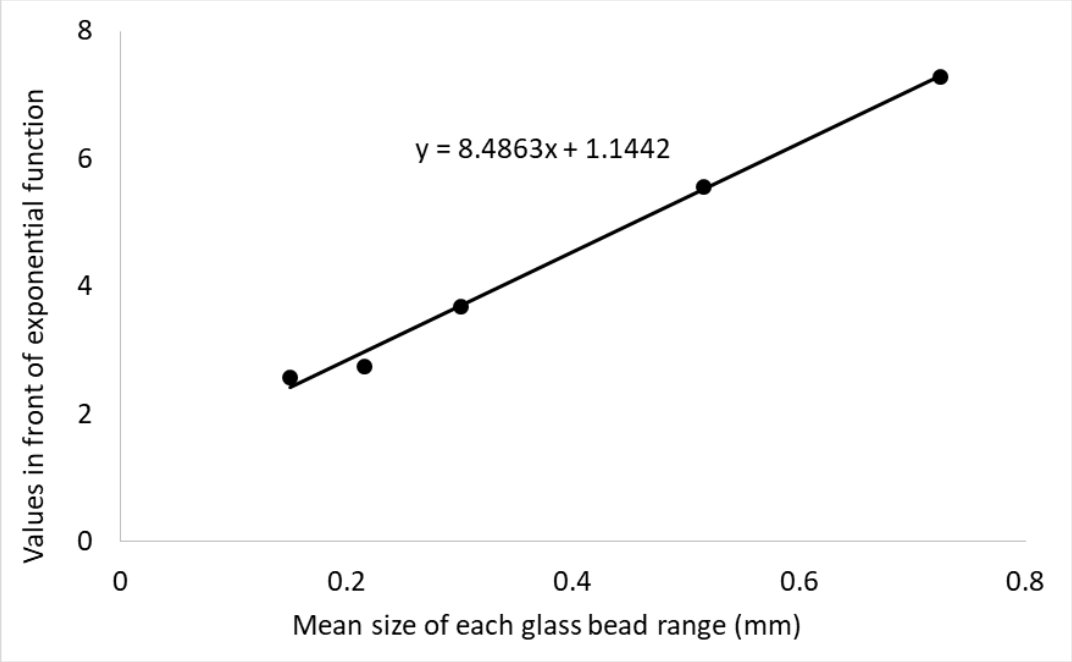

Figure 8: Values Leading the Power Functions vs. Bead Diameter.

A linear relationship was observed in Figure 8, and an equation to account for varying diameters of glass beads obtained. By combining this equation with the power function obtained in Figure 7, an empirical equation was derived.

$$y = (8.4863x + 1.1442)a^{-0.053} \quad (2)$$

Here, y is the predicted flow function value, x is the mean size of a glass bead range (mm), and a is the moisture percentage.

The percent error between experimental flow function values and the theoretical (using the empirical equation) was obtained. Notably, 0% moisture would not fit the model (as the output would be 0). The most accurate flowability values were instead obtained using a value of 10^{-16} % moisture content.

Table 3: Percent Error between Experimental and Theoretical Flow Function Values.

Glass Bead Diameter (mm)	Moisture Content			
	0%	1%	5%	15%
0.12-0.18	5.91%	11.1%	11.5%	1.08%
0.18-0.25	4.34%	3.00%	6.46%	16.0%
0.25-0.35	0.97%	3.75%	5.82%	7.49%
0.43-0.60	22.3%	23.5%	7.80%	13.7%
0.60-0.85	17.9%	3.85%	1.81%	6.38%

Table 3 shows an average error percentage of 8.73% accounting for all glass bead size ranges and moisture contents. The most error was obtained when including the 430-600 µm and 600-850 µm diameter ranges, which were observed in Figures 5d and 5e to perform poorly at higher moisture contents. Excluding these values, an average error percentage of 6.45% was obtained.

CHAPTER 4

CONCLUSIONS

As bead diameter was increased with no moisture content added, an increase in shear stress values at each value of applied normal stress was observed. Therefore, as material size is increased, higher values of applied shear stress are required for flow to begin. This corresponds with the flow function values seen in Table 1; as bead diameter size increased, the flow function (and therefore flowability) increased as well. Larger particles, therefore, flow better than smaller particles, but require more applied stress to begin to flow.

By testing materials with various levels of moisture content, it was observed that an increase in moisture content corresponds to an increase in applied shear stress values necessary for flow to begin. Inversely, as moisture content was increased, flow function was observed to decrease. Therefore, as moisture content increases, quality of flow decreases, and more applied stress is required to begin to flow. This holds true until 20% moisture content when the material becomes supersaturated; applied shear stress values drop below those observed at 15% moisture content, while the flow function value increases above that seen at 15% moisture content. These trends both correspond to those that would be expected from a liquid: higher quality flow and less stress required to begin to flow. These trends suggest that the material had become supersaturated with water at a value between 15% and 20% water-by-weight.

As seen in the empirical model, increasing glass bead diameter results in a linear increase in flowability, while flowability decreases as a power function with increasing moisture content. These relationships can be applied to the trends in slope observed at

varying bead diameters and moisture contents. The slope of shear stress vs. applied normal stress from dry material testing in Figure 4 increased noticeably as glass bead diameter was increased. Therefore, an increase in slope of shear stress vs. normal stress results in a linear increase in flow function. In contrast, wet material testing showed fairly consistent slope values at all moisture contents tested (particularly with sizes less than 430 μm; see Figures 5a, b, c, d, and e). In the empirical equation, the power function is to account for moisture content. Therefore, the presence of constant slopes of shear stress vs. normal stress as higher shear stress values are obtained corresponds to flow function decreasing as a power function.

An avenue for further research would be to investigate materials of different compositions in order to determine if any similarities exist in empirically-derived models. Furthermore, it would be beneficial to test sizes smaller than 120 μm, as the FT4 was observed to perform better with smaller material. The FT4 is only rated for materials with a diameter of less than 1000 μm; as this limit was approached (beads were tested up to 800 μm), significant standard deviation was observed between trials, especially amongst those with high quantities of water added. Sub-120 μm bead sizes may be more susceptible to static effects (attracting to both other particles and the vessel walls), which would be worth investigating with an antistatic solution. Ideally, the method of wet material preparation could be optimized; kneading in a Ziploc bag by hand cannot perfectly distribute moisture content, and so a more accurate model could be derived by improving material preparation methods. Also, the size distribution of each range of beads tested was not accounted for; the empirical equation assumed the mean value of

each size range, which certainly presented error. By confirming the distribution via sieving, a more accurate model could be obtained.[5]

REFERENCES

[1] Osborne, Ben. “Powder Testing: Shear Cell.” *Powder Testing with the FT4 Powder Rheometer*, Freeman Technology, 2018, www.freemantech.co.uk/_powders/powder-testing-shear-cells.

[2] “Granular Materials.” *Complex Systems: UCSB Physics*, University of California, Santa Barbara, 2018, web.physics.ucsb.edu/~complex/research/granular.html.

[3] C. Hare, U. Zafar, M. Ghadiri, T. Freeman, J. Clayton, M.J. Murtagh (2015). Analysis of the dynamics of the FT4 powder rheometer. Powder Technology, Volume 285, 123-127, ISSN 0032-5910.

[4] Scicolone, J., Metzger, M., Koynov, S., Anderson, K., Takhistov, P., Glasser, B., & Muzzio, F. (2016). Effect of liquid addition on the bulk and flow properties of fine and coarse glass beads. AIChE Journal, 62(3), 648-658.

[5] Kleppe, Cameron. “Shear Stress Properties of Granular Materials.” (2018).

[6] Flowchart Maker & Online Diagram Software. https://www.draw.io/ (accessed Oct 20, 2019).

[7] Rhodes, M.J. *Introduction to Particle Technology*. New York: John Wiley & Sons; 1998. p. 265–292.

[8] Çagli, A.S. & Devec, B.N. & Okutan, C.H. & Rkec, D.A.A. & Teoman, E.Y.. (2007). Flow property measurement using the Jenike shear cell for 7 different bulk solids. Proc. Eur. Congr. Chem. Eng. (ECCE-6) Copenhagen. 16-20.

[9] Mehos, G.; Eggleston, M.; Grenier, S.; Malanga, C.; Shrestha, G.; Trautman, T. (2018). Designing Hoppers, Bins, and Silos for Reliable Flow. Chem. Eng. Prog., 114 (4).

APPENDIX A

MOHR'S CIRCLES USED FOR FLOW FUNCTION CALCULATION

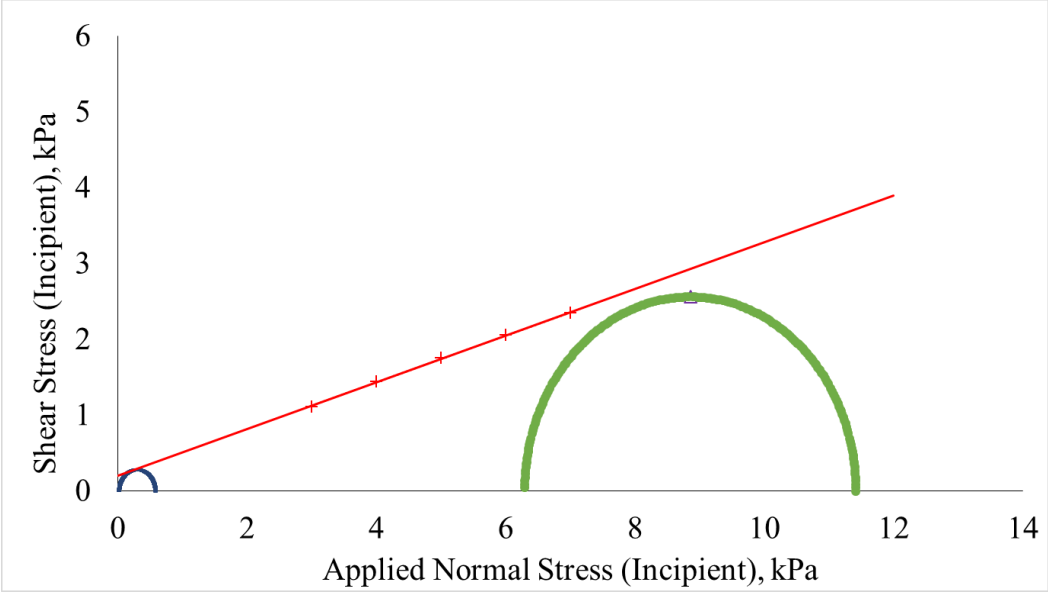

Appendix A Figure 1: Mohr's Circles for 120-180 µm beads with 0% moisture.

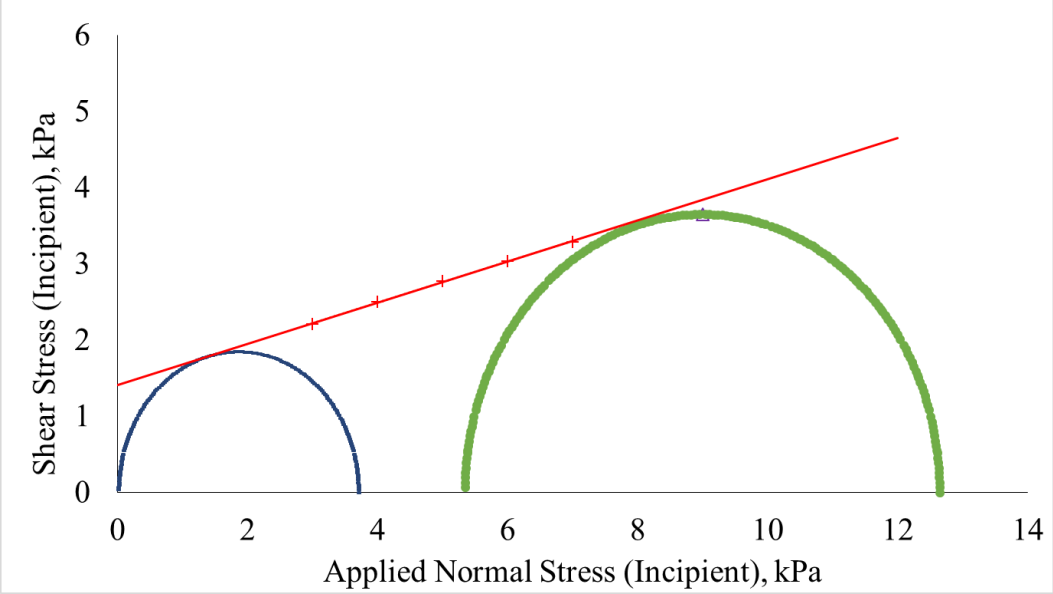

Appendix A Figure 2: Mohr's Circles for 120-180 µm beads with 1% moisture.

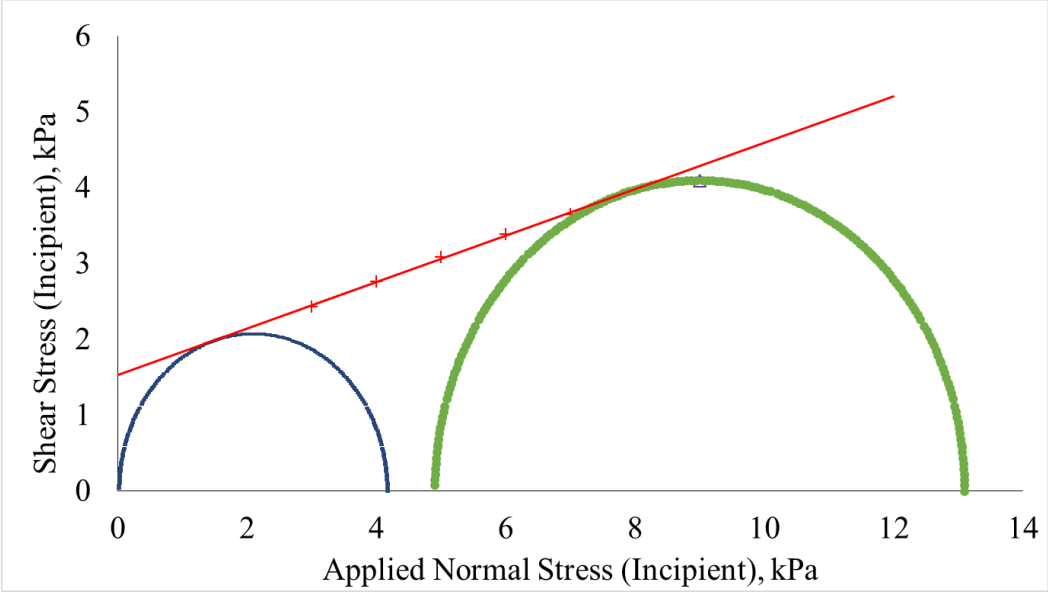

Appendix A Figure 3: Mohr's Circles for 120-180 µm beads with 5% moisture.

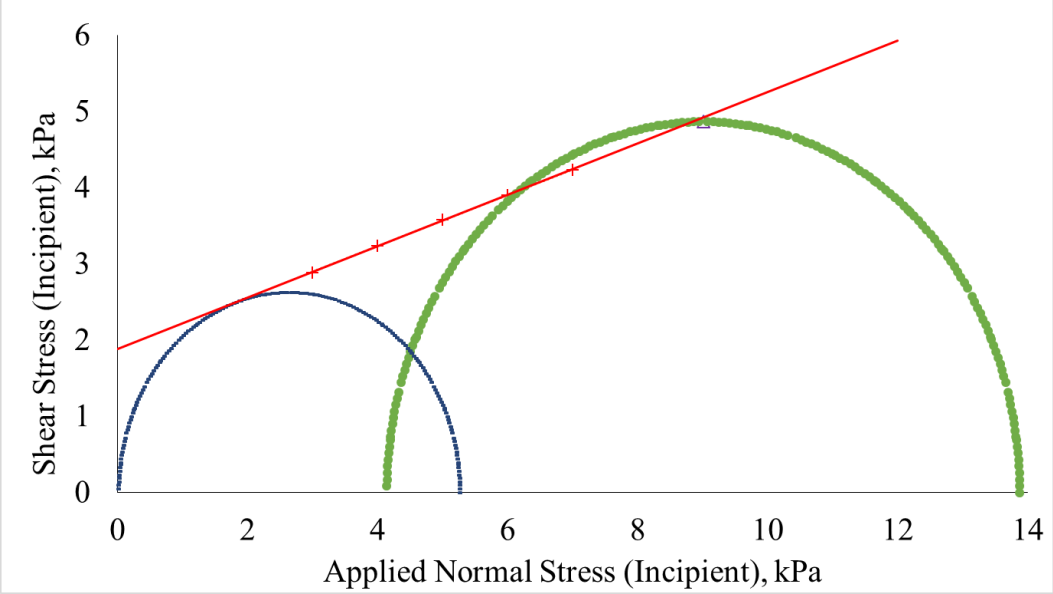

Appendix A Figure 4: Mohr's Circles for 120-180 µm beads with 15% moisture.

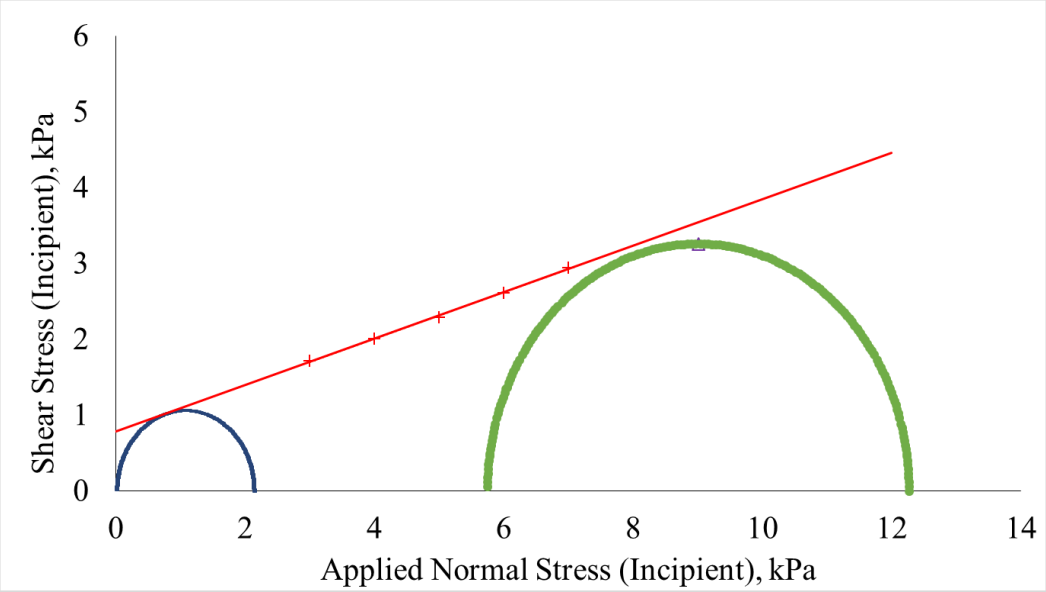

Appendix A Figure 5: Mohr's Circles for 120-180 µm beads with 20% moisture.

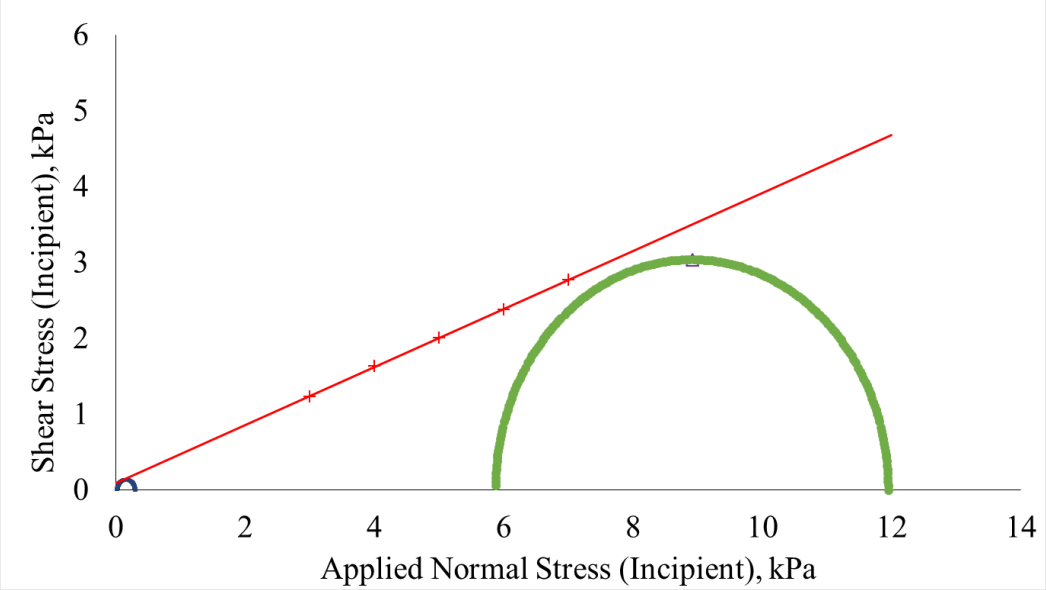

Appendix A Figure 6: Mohr's Circles for 180-250 µm beads with 0% moisture.

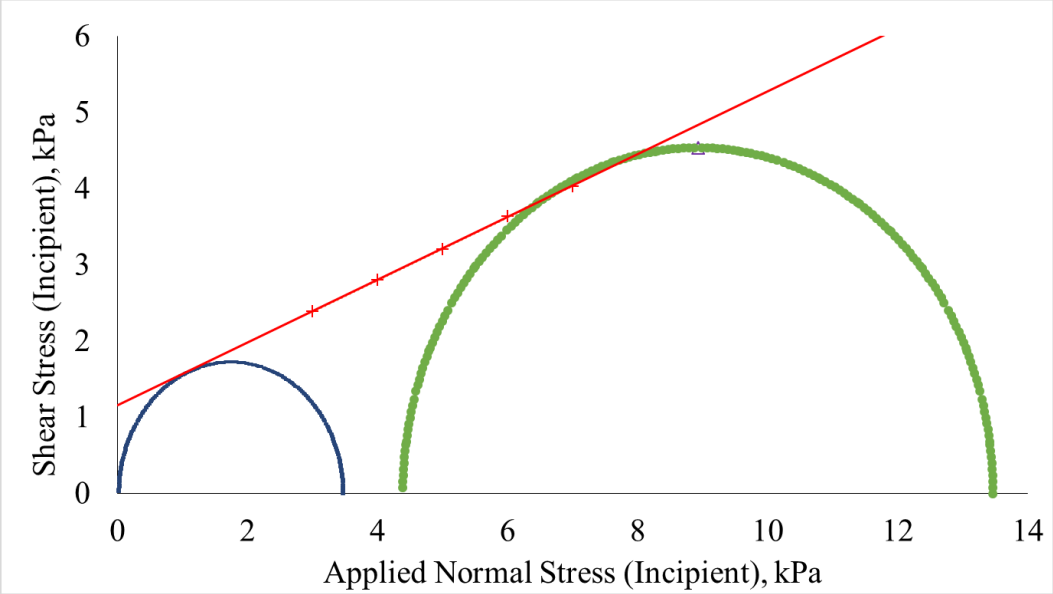

Appendix A Figure 7: Mohr's Circles for 180-250 µm beads with 1% moisture.

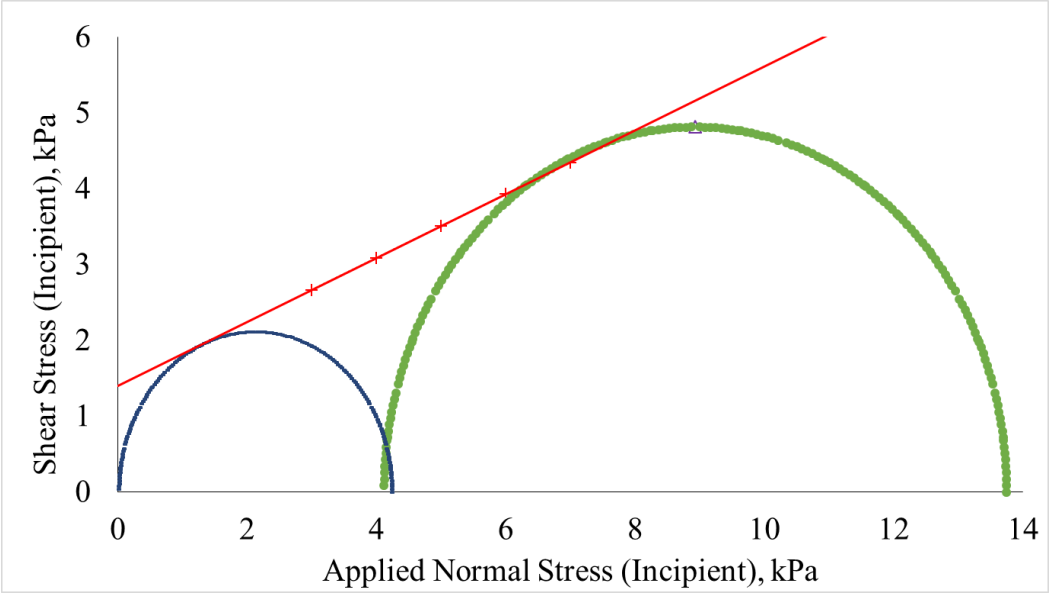

Appendix A Figure 8: Mohr's Circles for 180-250 µm beads with 5% moisture.

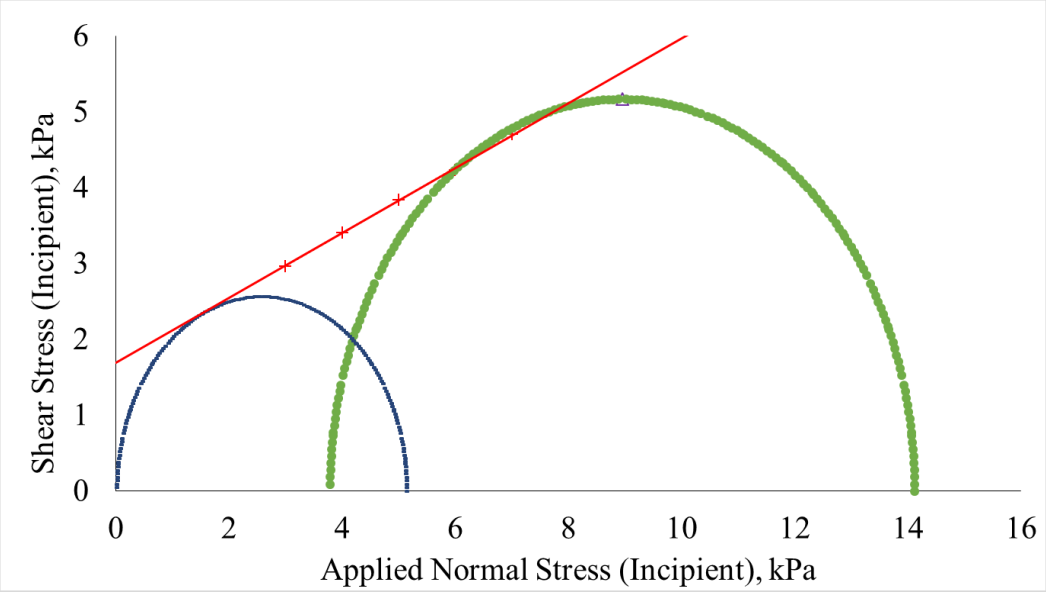

Appendix A Figure 9: Mohr's Circles for 180-250 µm beads with 15% moisture.

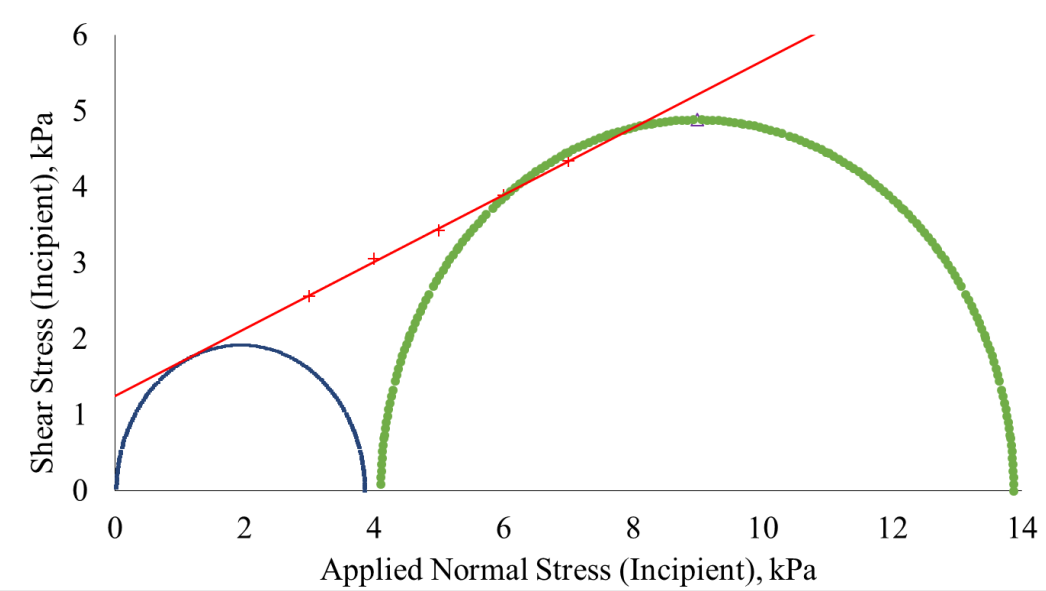

Appendix A Figure 10: Mohr's Circles for 180-250 µm beads with 20% moisture.

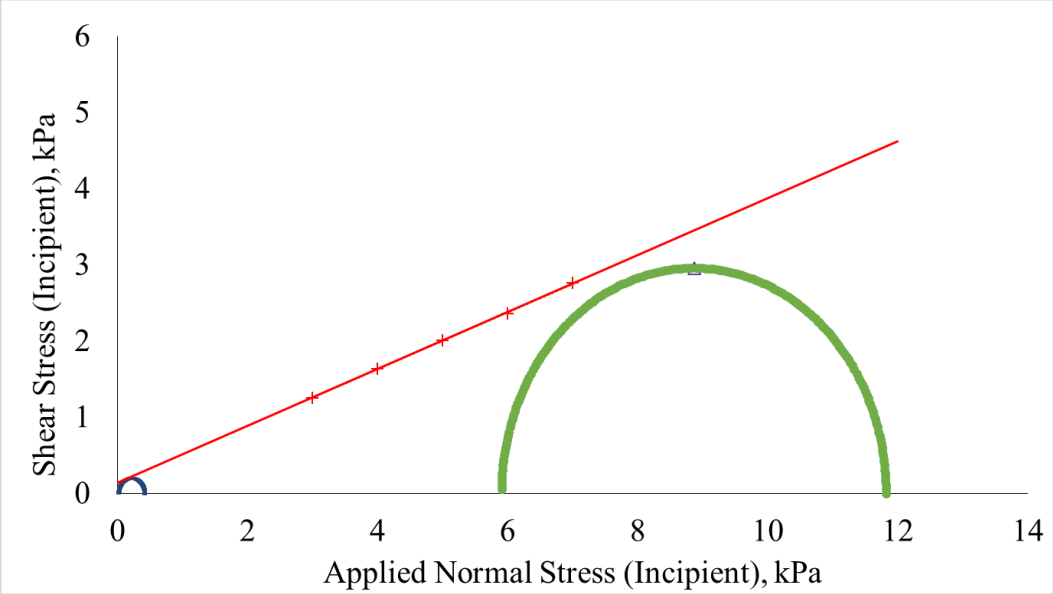

Appendix A Figure 11: Mohr's Circles for 250-350 µm beads with 0% moisture.

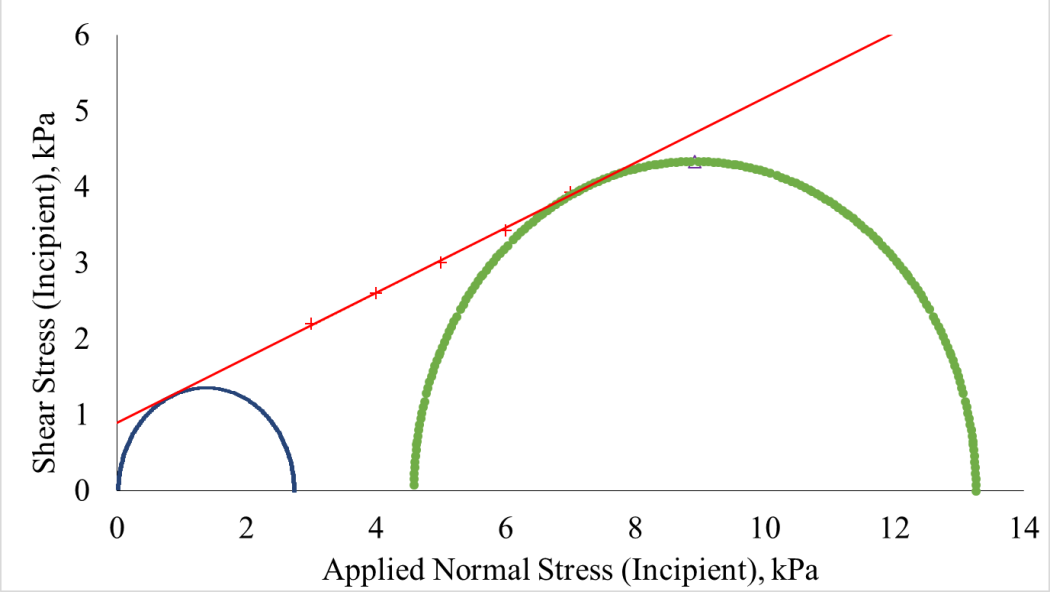

Appendix A Figure 12: Mohr's Circles for 250-350 µm beads with 1% moisture.

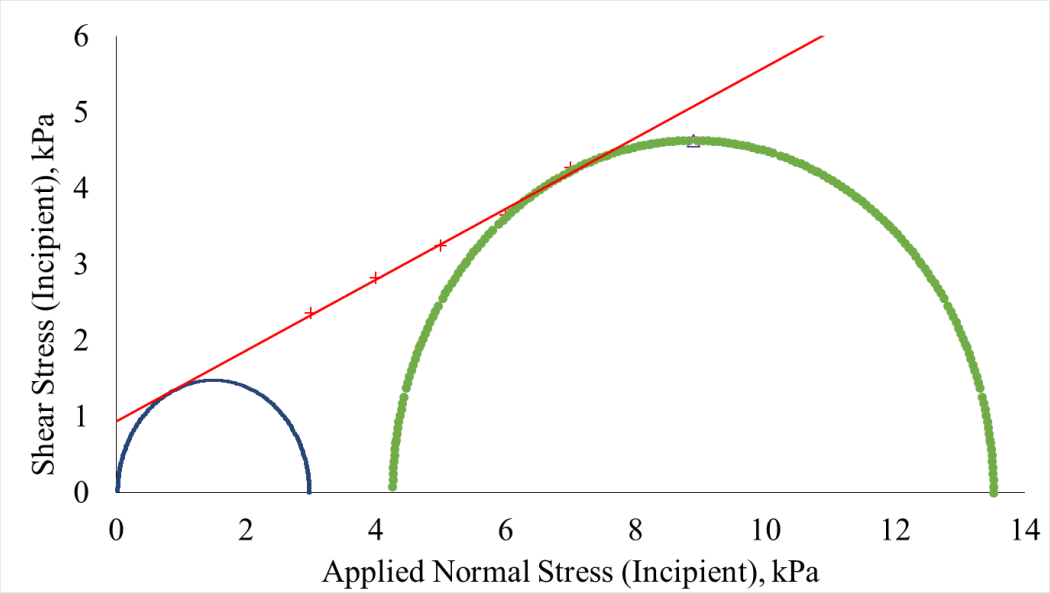

Appendix A Figure 13: Mohr's Circles for 250-350 µm beads with 5% moisture.

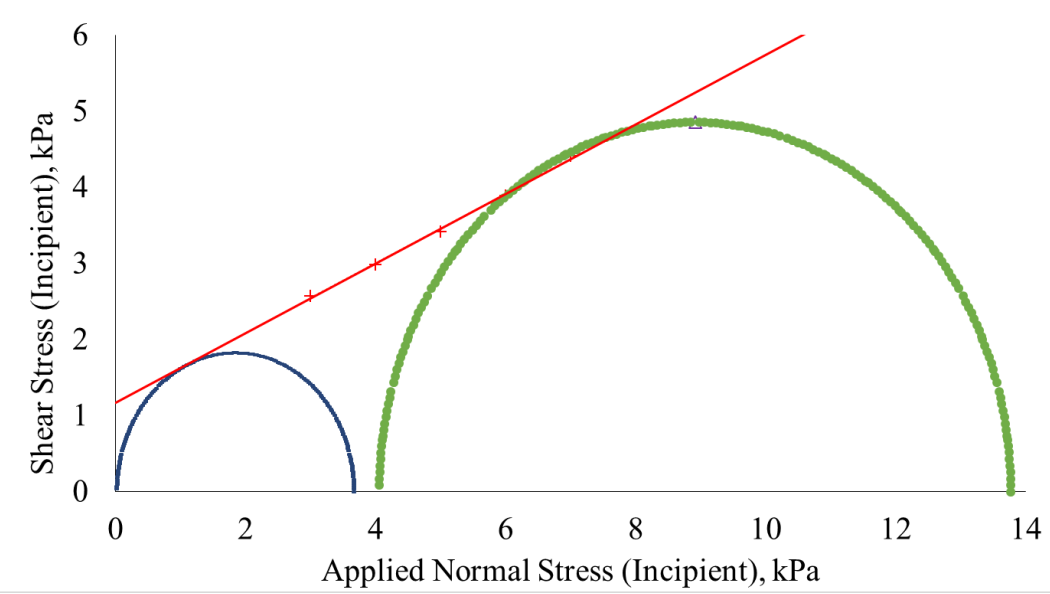

Appendix A Figure 14: Mohr's Circles for 250-350 µm beads with 15% moisture.

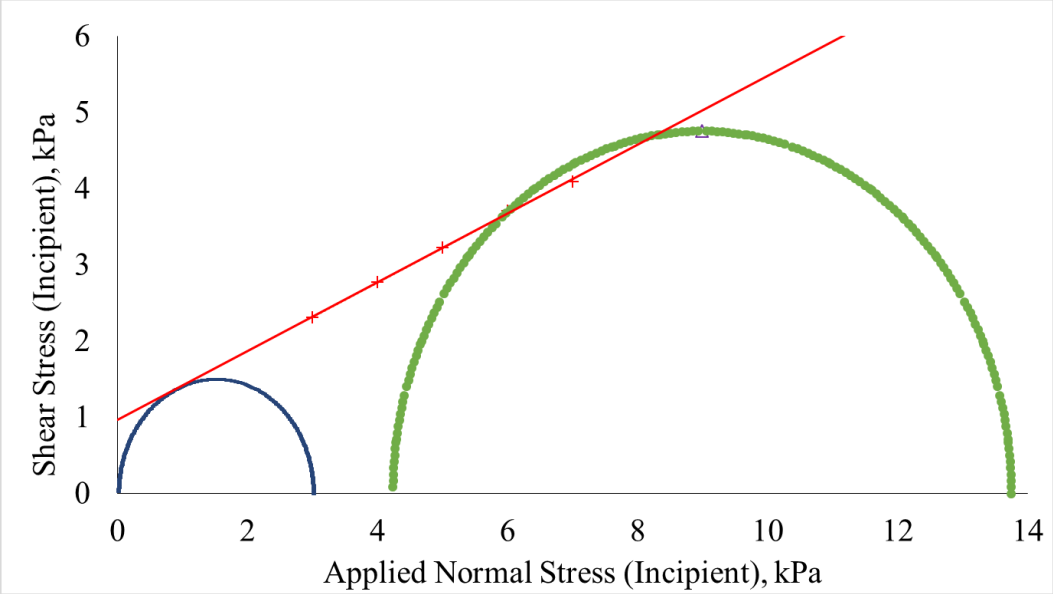

Appendix A Figure 15: Mohr's Circles for 250-350 µm beads with 20% moisture.

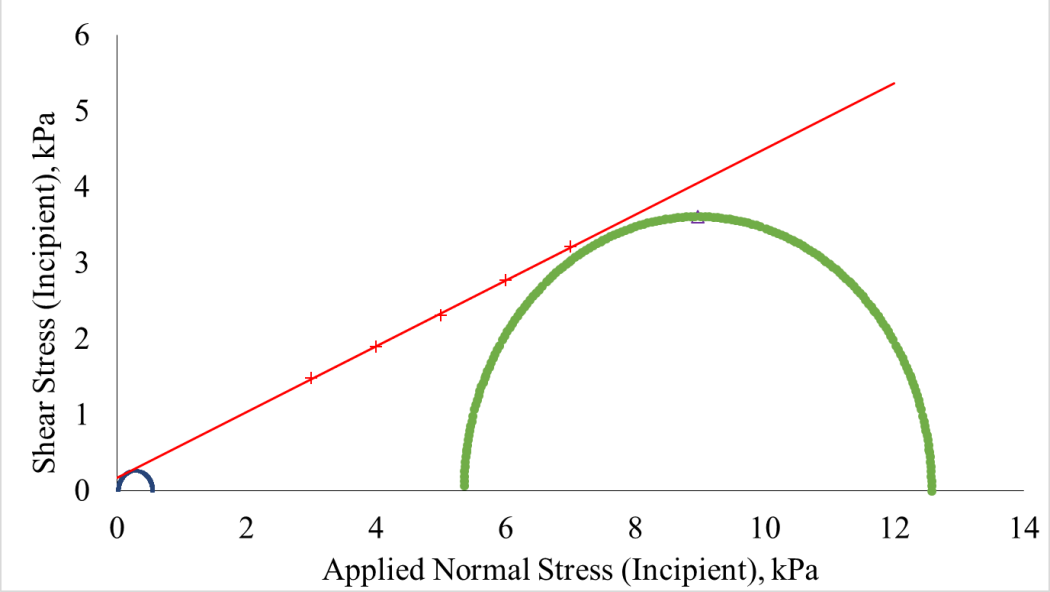

Appendix A Figure 16: Mohr's Circles for 430-600 µm beads with 0% moisture.

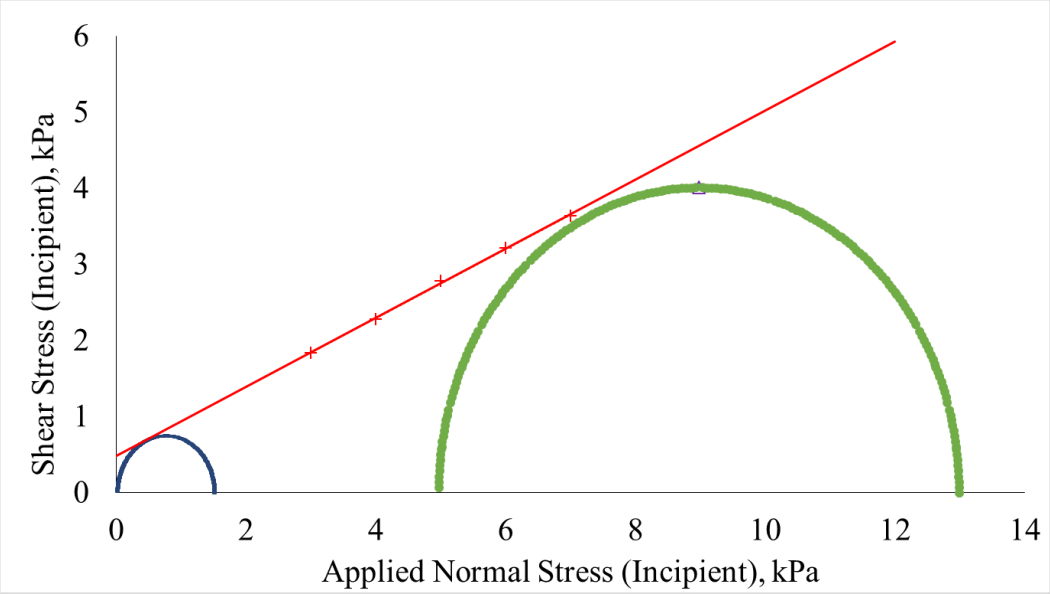

Appendix A Figure 17: Mohr's Circles for 430-600 µm beads with 1% moisture.

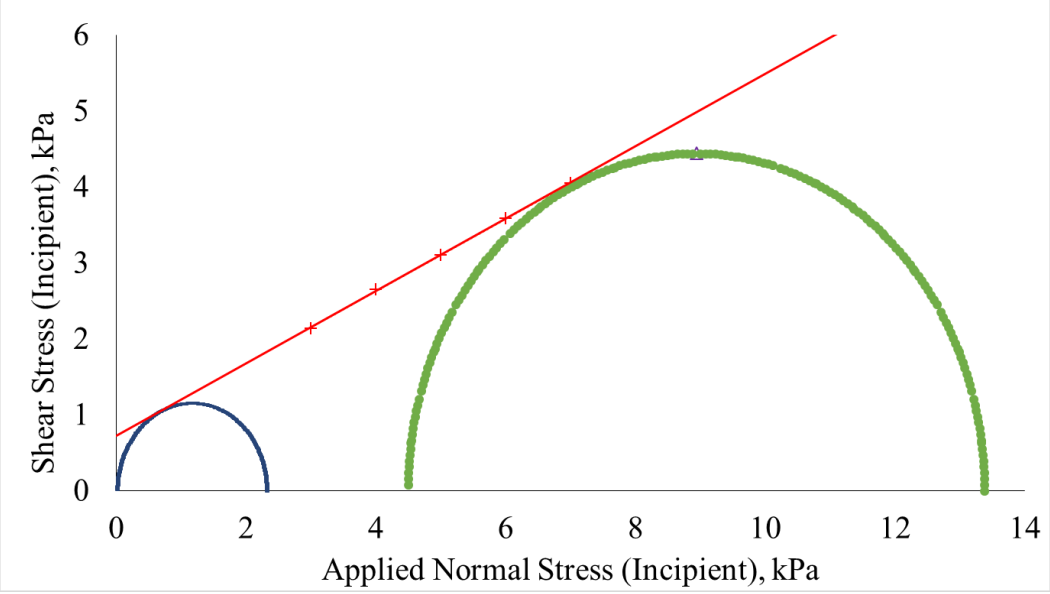

Appendix A Figure 18: Mohr's Circles for 430-600 µm beads with 5% moisture.

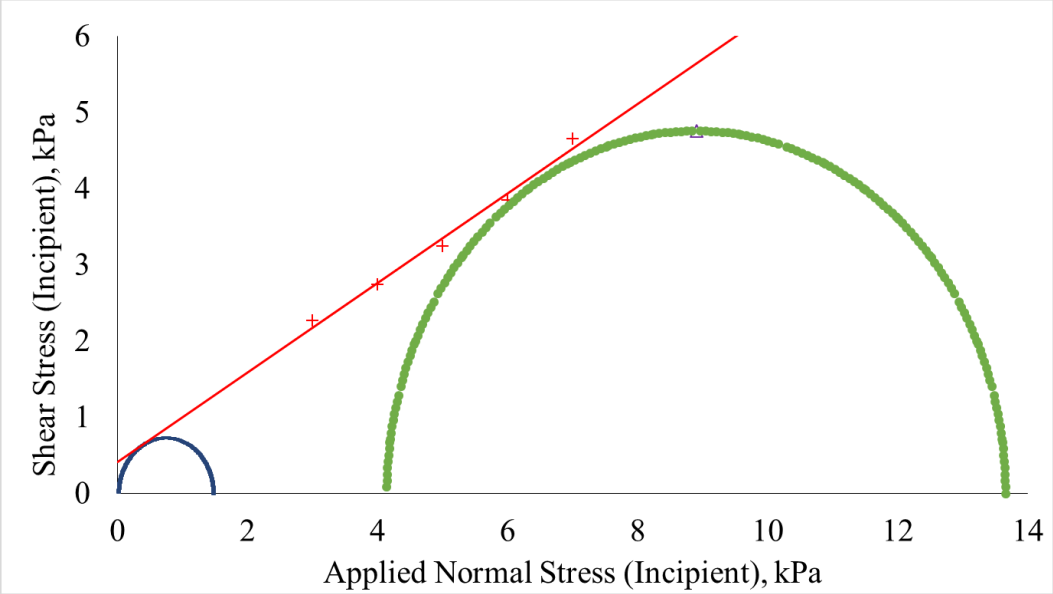

Appendix A Figure 19: Mohr's Circles for 430-600 µm beads with 15% moisture.

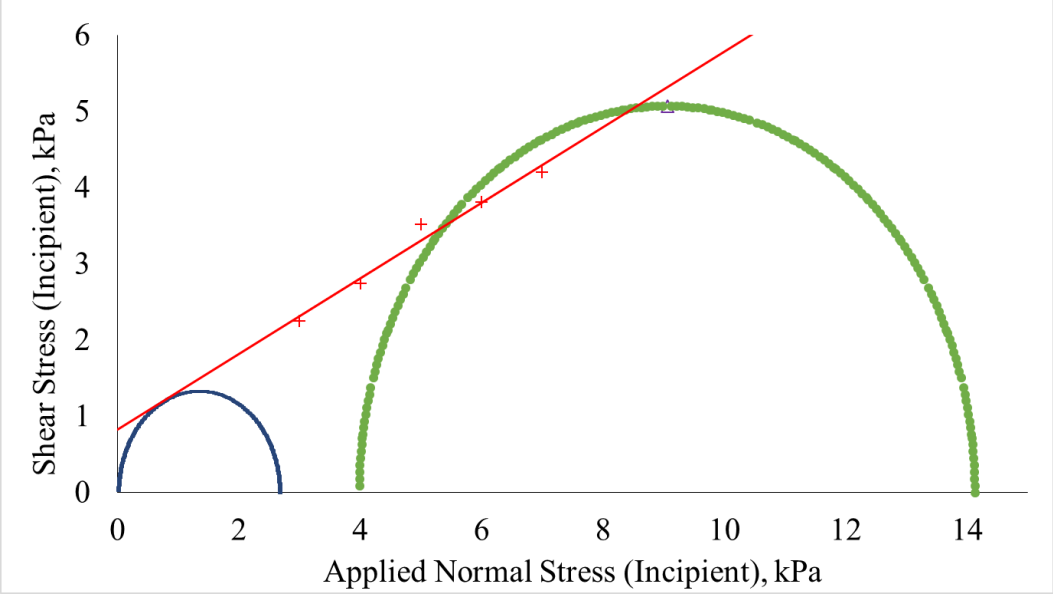

Appendix A Figure 20: Mohr's Circles for 430-600 µm beads with 20% moisture.

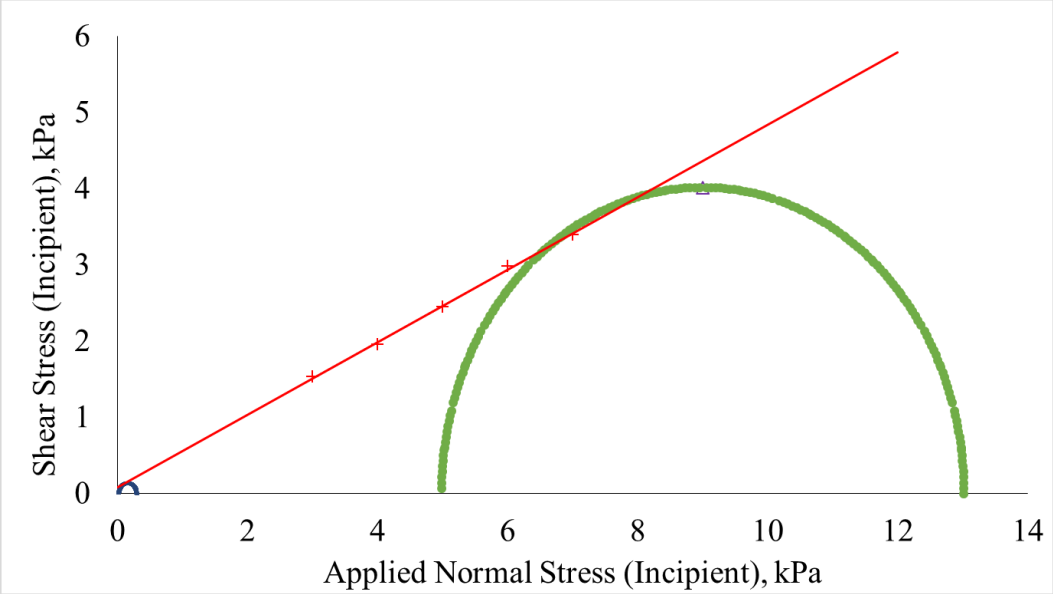

Appendix A Figure 21: Mohr's Circles for 600-850 µm beads with 0% moisture.

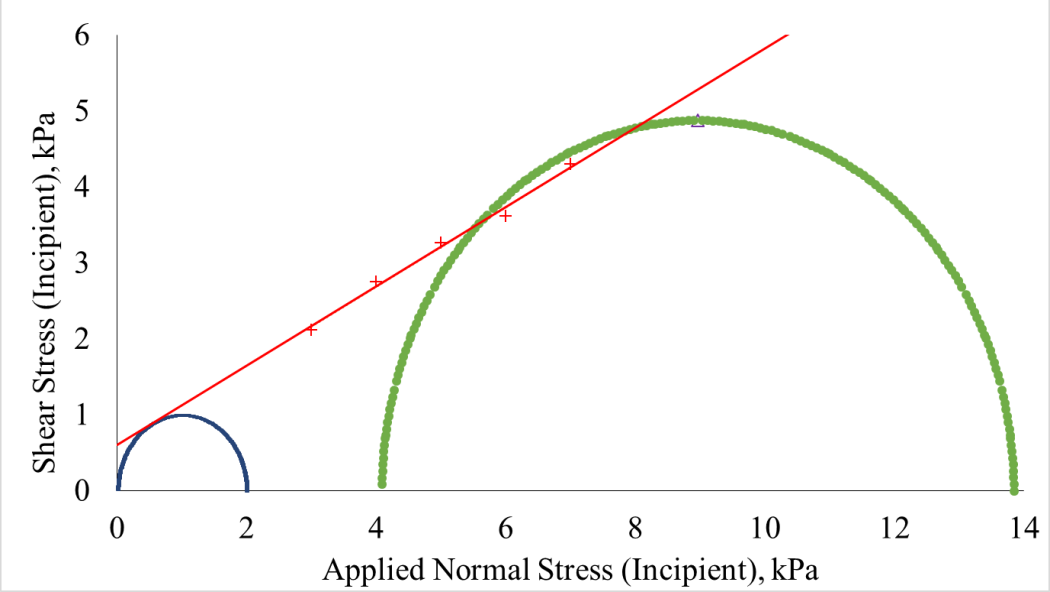

Appendix A Figure 22: Mohr's Circles for 600-850 µm beads with 1% moisture.

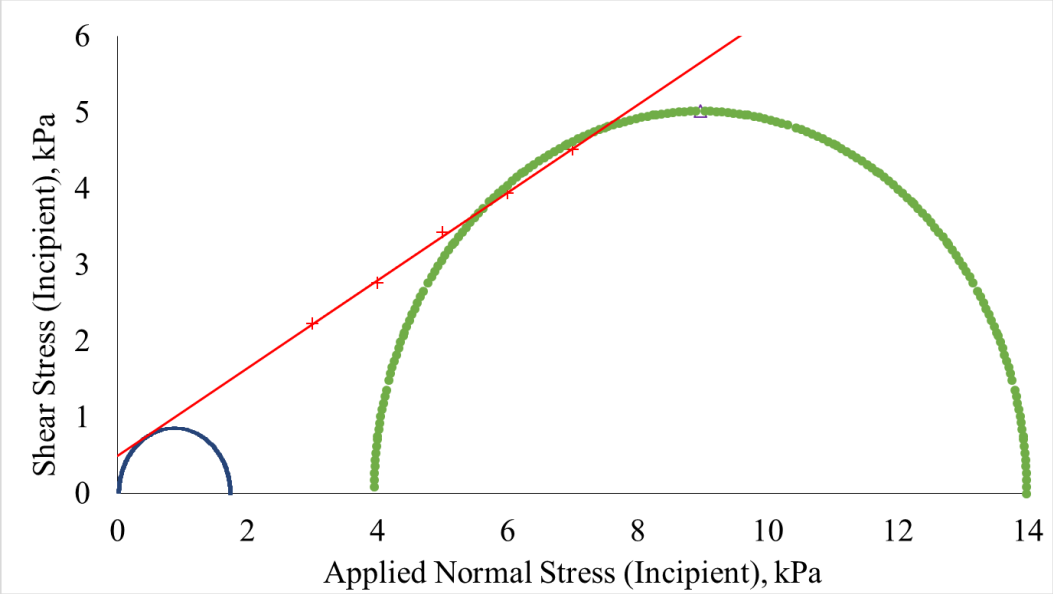

Appendix A Figure 23: Mohr's Circles for 600-850 µm beads with 5% moisture.

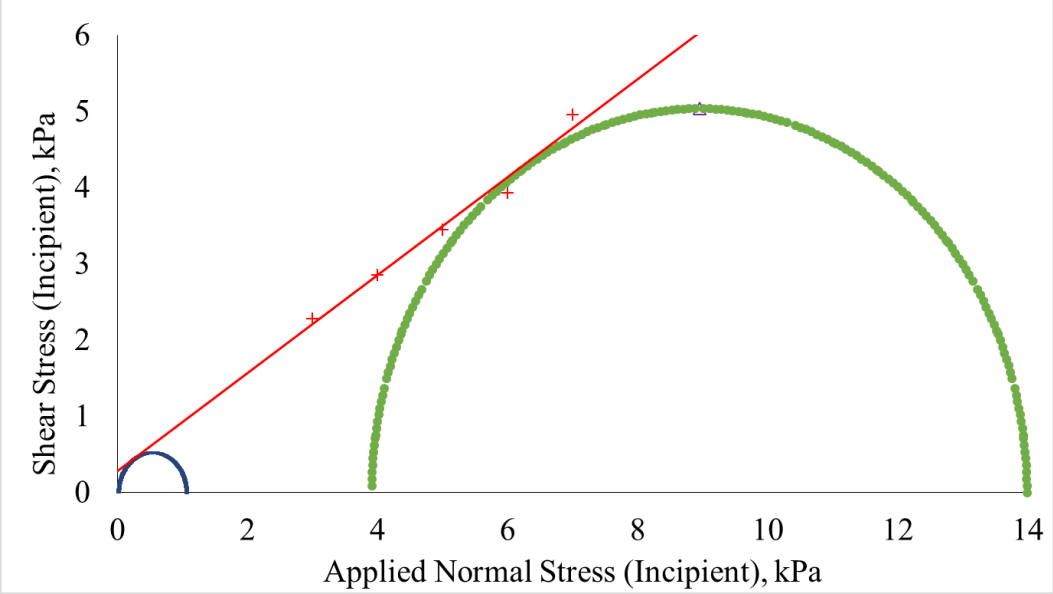

Appendix A Figure 24: Mohr's Circles for 600-850 µm beads with 15% moisture.

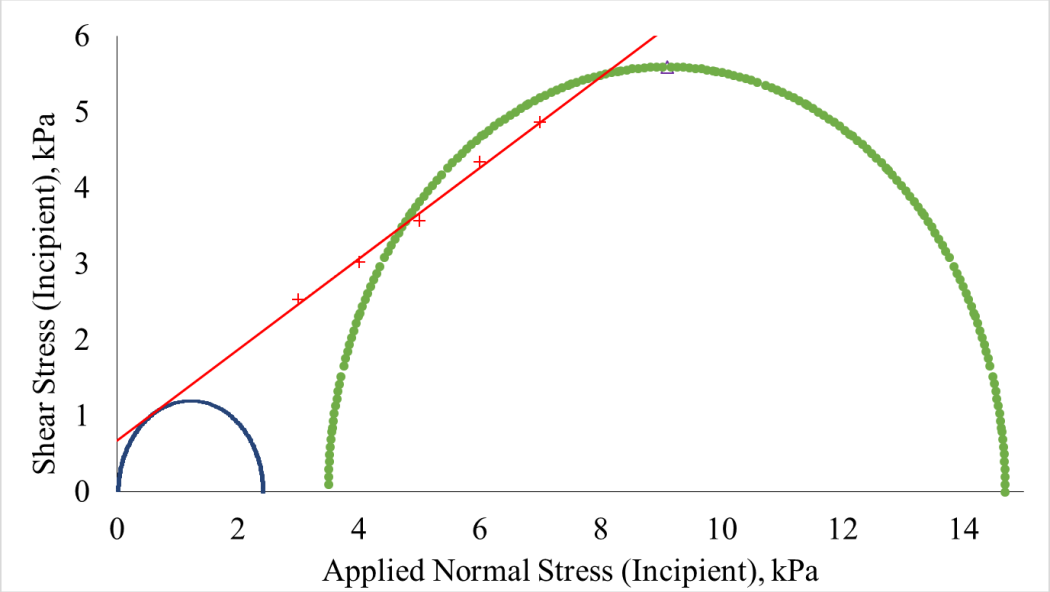

Appendix A Figure 25: Mohr's Circles for 600-850 µm beads with 20% moisture.